



Tectonic control and geometric characterization of hydrothermal vent confession of hydrothermal vent complex using seismic data, Potiguar Basin - Brazil OF A HYDROTHERMAN 3 Lorenna Sávilla Brito Oliveira¹, Luiza Cavalcante Vinhas Lucas¹, David Iacopini², Fabrizio Balsamo³, Anita Torabi⁴, Behzad Alaei⁵, João Felipe de Sousa Neto¹, Pedro 5 Edson Face Moura⁶, David Lino Vasconcelos⁷, Vincenzo La Bruna¹, Francisco Hilário Rego Bezerra¹ 6 1 Postgraduate Program in Geodynamics and Geophysics, Federal University of Rio 8 Grande do Norte (UFRN), Campus Universitário - Lagoa Nova, CEP 59078-970, Natal, 9 Rio Grande do Norte, Brazil. 10 2 Department of Earth, Environmental and Resource Sciences (DISTAR - Dipartimento di Scienze della Terra, dell'Ambiente e delle Risorse), University of Naples Federico II, 11 12 Naples, Italy. 13 3 Department of Chemistry, Life Sciences, and Environmental Sustainability, University of Parma, Parma, Italy, 14 15 4 Department of Geosciences, University of Oslo, Postboks 1047, Blindern 0316, Oslo, Norway. 16 17 5 Earth Science Analytics, Strandveien 3333, 1366 Lysaker, Norway. 18 6 Postgraduate Program in Geology, Federal University of Ceará (UFC), Campus do 19 Pici, Bloco 912, CEP 60440-900, Fortaleza, Ceará, Brazil. 7 Federal University of Campina Grande (UFCG), Aprígio Veloso, 882, Campus 20 21 Universitário, Campina Grande, Paraíba, CEP 58429-900, Brazil. 22 Correspondente to: Lorenna Oliveira (lorenna savilla@hotmail.com) 23 **ABSTRACT** 24 25 Hydrothermal vent complexes in sedimentary basins are linked to igneous intrusions, which induce structural and thermal perturbations, causing forced 26 27 folds, hydrocarbon maturation, and fluid remobilization. While their genesis is 28 often associated with magmatic heat and hydraulic fracturing, the controlling 29 factors of their geometry and development remain debated. This study analyzes 30 3D seismic data from the Potiguar Basin (onshore Brazil), identifying vent structures, two of which were extracted in a 3D perspective from the variance 31 attribute. Our results indicate that all the vents are structurally controlled 32 33 by regional-scale faults, which enhance permeability starting from the hydraulic REALISTIC





fracturing and boiling processes. Seismic attributes, such as variance and dip 34 illumination have proven effective in identifying vent structures, fault associations, 35 and fluid pathways, providing insights into their spatial distribution and geometric 36 characteristics. Cosine of phase attribute reveals that hydrothermal vents exhibit 37 varying geometries as they cut different sedimentary units within the basin. Our 38 findings highlight the petrophysical implications of a fault zone in a hydrothermal 39 vent complex and advance understanding of silicification processes in 40 sedimentary reservoirs. 41 Keywords: Hydrothermal vents, seismic attributes, fault zones, fluid migration, 42 sedimentary basins. 43

1. INTRODUCTION

44

45

Hydrothermal vents are a complex combination of elements that 46 potentially affect the petrophysical properties of reservoirs. They have been 47 described in sedimentary basins associated with volcanic activities as injections 48 of igneous plumbing systems, dikes, and sills (Skoseid et al., 1992; White and 49 McClintock, 2001; Svensen et al., 2003; Jamtveit et al., 2004; Planke et al., 2005; 50 ? WHICH? VENTS OR INTRUSEMS? Hansen et al., 2008)/These igneous injections are known to induce structures as 51 forced folds, hydrofracturing systems, and seals. They also behave as 52 hydrocarbon traps (Hansen and Cartwright, 2006; Jackson et al., 2013), causing 53 early maturation of hydrocarbons (Kennish et al., 1992; Hansen and Cartwright, 54 2006), increasing the hydrothermal aureole width (Svensen et al., 2004), and 55 remobilizing sand and fluid pipes (Svensen et al., 2006; Jamtveit et al., 2004). All 56 volcanic processes create disturbances in the reservoirs, forming 57 hydrothermal vents with various architectures that relocate gas, mixed fluids, and 58

ODD MEANING ?

O VENTS #

6 RESERVOURS?

RESERVOIRS?

(3) NO VOLCANIE.



62

63

64

65

66

67

74

75

76

77

78

79

80

81

82

83



hot waters (Svensen et al., 2003; Procesi et al., 2019; Finn et al., 2022; Rovere et al., 2022).

7 RELEVANCE.

The hydrothermal vents are associated with igneous intrusions

However, the intrusive processes and rock parameters that control the pathways and conduit architectures of these structures remain poorly understood, as most interpretations are based on post-mortem eismic data analysis (Cartwright,

2010; Jamtveit et al., 2004; Planke et al., 2005; Svensen et al., 2006; Moss and

Cartwright, 2010b). The major uncertainty refers to what triggers the hydraulic

fracturing mechanisms that guide the nucleation and then propagation of the vent

68 formation. Other than intrusive systems, hydrothermal vents have been described

69 as developed by synsedimentary processes, or erosive fluidization (McDonnell et

al., 2007). Depending on the type of sills, intrusions trigger the overpressure region (Svensen et al., 2006; Davies et al., 2012; Alvarenga et al., 2016). Other

72 uncertainties relate to the vent interactions with the seabed cap depending on its

73 geological nature and stratigraphy (Moss and Cartwright, 2010b).

In vent complexes, the main pathways have been described by fluid escape structures named fluid pipes, characterized by highly localized vertical to sub-vertical pathways of focused fluid venting from some underlying source region. The term fluid pipe was used as synonymous of gas chimney triggered by a pressure cell, composed of a gas or mud source (Svensen et al., 2006). In literature, the geometry of vents (both methane or hydrothermal) has been classified based on cross-sectional and plan-view characteristics as domeshaped, eye-shaped, and crater forms (Planke et al., 2005; Cartwright and Santamarina, 2015) (Fig. 1B). The relationship between vent boundaries and surrounding strata have been defined, focusing on concordant, divergent, or

B PORT- MORTEM Some seizmic OUTA IMAGE ACTIVE VENTS...

KIRKHAM ETAL.

AND OTHERS

HAVE

ADDRESSED

THIS ASPECT.

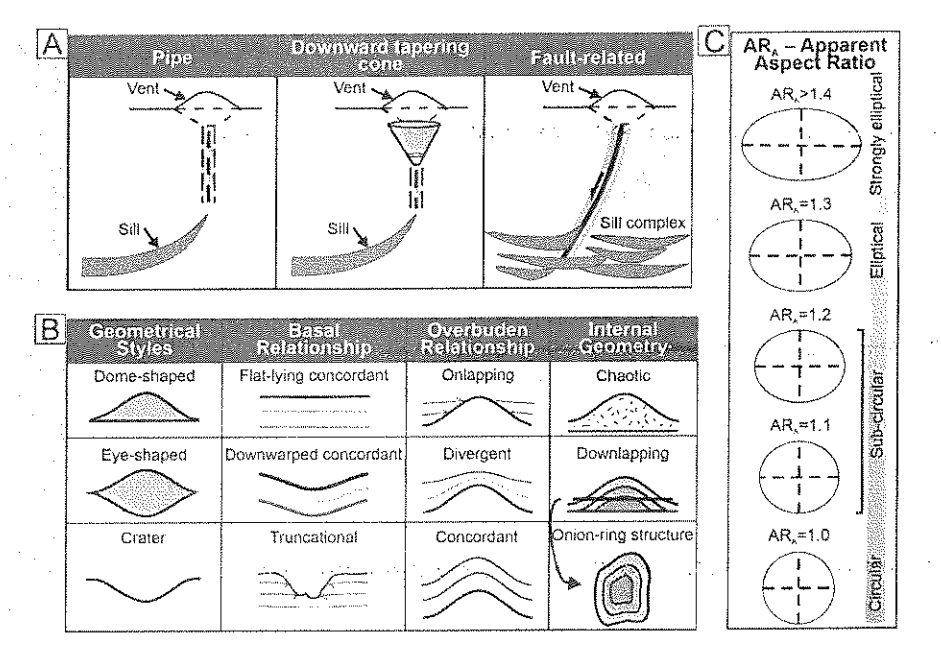




truncated patterns (Fig. 1B), but also using the internal reflections within vents 84 (Hansen, 2006). In seismic data, vents (no matter their origin) can be measured 85 by the diameters and lengths of conduits, checking the connections between sill 86 terminations and upper vent regions identified as cylindrical zones of disturbed 87 seismic data (Hansen, 2006; Maestrelli et al., 2017) (Fig. 1A and Fig. 1C).

89

88



15 THIS A LITERATURE review of A THESIS? IT GOES AROUND IN CIRCLES ...

Figure 1 - Vent geometric parameters related to the external (A) and internal (B) shapes and the Apparent Aspect Ratio classification (C) related to the pipes ratio in a map view, which expresses the variation between circular to strongly elliptical shapes. (A), (B) and (C) were modified from Hansen et al (2006), Planke et al (2005), and Maestrelli et al (2017).

99

100

101

90

91

92

93

94

In all those contexts, seismic data represent a useful tool for identifying hydrothermal vents in several sedimentary basins (Planke et al., 2005; Hansen, 2006; Cartwright and Santamarina, 2015; Alvarenga et al., 2016; Kjoberg et al., 2017; Omosanya et al., 2018; Wang et al., 2019; Mituku and Omosanya, 2020).



c) 123



Seismic attributes have been applied to reveal hydrothermal chimneys, vents, and structures around them, such as faults, fractures, folds, and sag structures (Jackson et al., 2013; Plaza-Faverola et al., 2015; Omosanya et al., 2018; Rovere et al., 2022). Vents associated with preexisting structures have also been previously described as ducts forming at the tops of faults and classified as the 'fault-related' (Hansen, 2006; Maestrelli et al., 2017; Wang et al., 2019). These vents typically exhibit a vertical pipe-like shape with a dome or mound at the top (Alvarenga et al., 2016; Magee et al., 2016). Coherence attributes and instantaneous phase were used to highlight the sag collapse structures associated with polygonal faults, vents related to crestal faults, and fault-controlled vents (Hansen, 2006; McDonnell et al., 2007; de Mahiques et al., 2017; Omosanya et al., 2018; Mituku and Omosanya, 2020). However, these attributes applied as tools for identifying vent complex geometry failed to recognize lateral fluid injection features and hydrofractures.

NOT REALLY NOVEL

Across several hydrothermal vent complexes, the mechanisms of propagation and the processes of nucleation remain poorly understood. Key scientific uncertainties include whether hydrothermal vent propagation is linked to preexisting fault zones, the extent to which the final architecture is controlled by fault systems, and whether some hydrothermal vents are entirely dependent on overpressure-driven intrusive mechanisms. Another important consideration is whether fault zones can later re-exploit the existing architecture of hydrothermal vents. Additionally, the influence of host rock properties on the development of vent architecture remains an open topic for investigation.

NOT SOMETHING YOU CAN ADDRESS WITH SEISMIC DRIA

To answer the above questions, we selected the onshore part of the Potiguar Basin, where previous studies identified outcrops with hydrothermal

Sosanc.





silicification related to faults (Menezes et al., 2019). This study aims to describe and characterize the architecture and surrounding structures of hydrothermal vents using 3D onshore seismic data from the Potiguar Basin. We identified and seismically characterized 3 hydrothermal vents and 9 fluid pipes using seismic attributes and extracted geobodies from 2 of them to better interpret their internal architecture. Our interpretations suggest that all the hydrothermal vents are associated with regional-scale faults, with their lateral extensions related to fluids affecting sedimentary formations. The mapped structure suggests faults provide the structural permeability, enhanced by the hydraulic fracturing, and leading to the formation of hydrothermal vents. The result of this study contributes to a better understanding of the hydrothermal vent propagation mechanism and silicification process in sedimentary successions.

BY VERY
SAMEL
DATA SET.

SEE
C. EIRK HAM (NILE)
C. ROELDFISE (NORWAY +
GULF OF MEXICO)
+ MARCINE (NEOLOGY
PARERS

2. GEOLOGICAL SETTINGS

The Potiguar Basin is situated in the Brazilian Equatorial Margin (Pessoa Neto et al., 2007) (Fig. 2). This passive margin basin formed during the Early Cretaceous and exhibits a structural framework characterized by half-grabens and horsts bounded by fault systems that reactivated shear zones in the crystalline basement (Matos, 1992, 1999; de Castro et al., 2012). Its evolution comprises three main depositional supersequences: rift, post-rift, and drift, corresponding to distinct tectono-sedimentary phases (Bertani et al., 1990; Pessoa Neto et al., 2007).



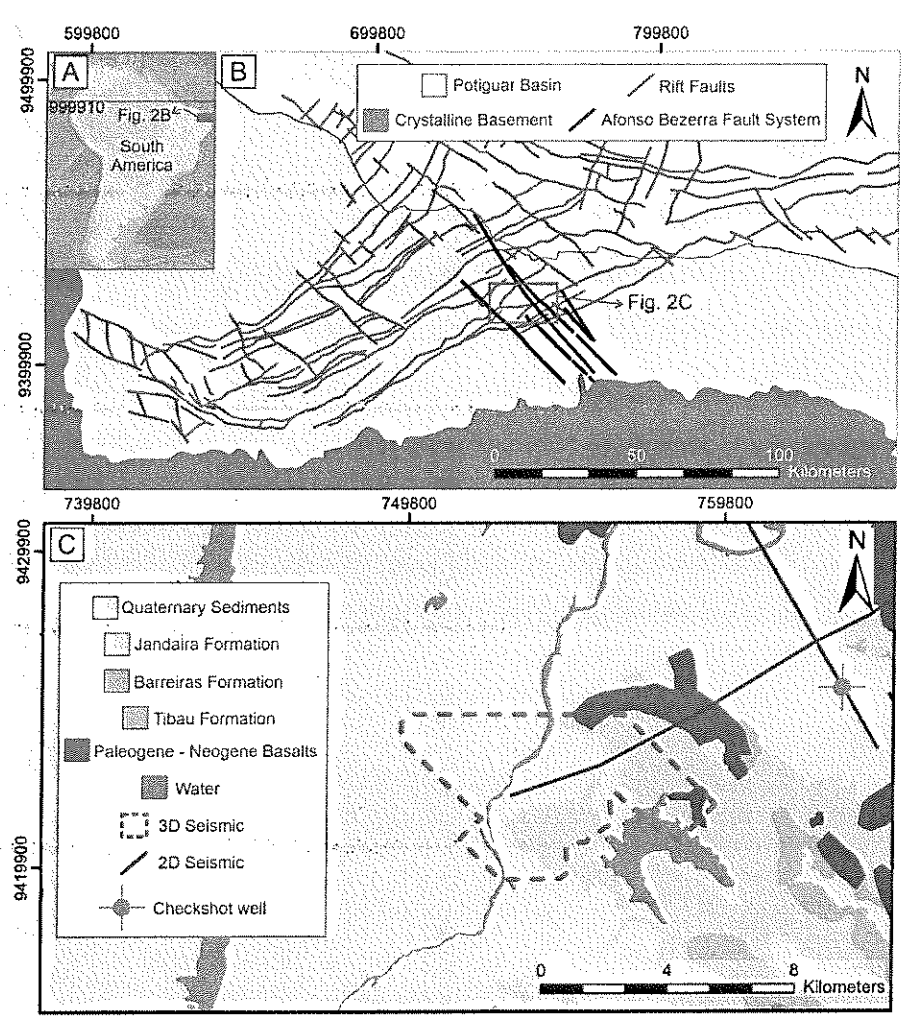


Figure 2 - (A) Study area located on the South American continent. (B) Geological map of the Potiguar Basin and (C) the study area with lithologies, and the seismic and well data location. Modified from Bertani et al. (1990), Bezerra et al. (2009), de Castro and Bezerra (2015).

56

The Potiguar basin rift phase coincides with the initial breakup of Pangea and the opening of the South Atlantic (de Castro, 2011; de Castro et al., 2014). This phase began during the early Valanginian, a stage characterized by intense crustal stretching, resulting in mechanical subsidence and the formation of





grabens (Araripe and Feijó, 1994; Fonseca et al., 2024). In this phase, the main structure was the Carnaubais fault system, striking NE-SW and dipping E-W, which resulted from the brittle reactivation of the Portalegre shear zone in the basement (de Castro et al., 2012). The creation of grabens and horsts is related to NE-SW-oriented linear features (Bertani et al., 1990). NW-SE-oriented transfer and accommodation faults controlled the southern edge of the rift, displacing the NE-SW-oriented faults in the Potiguar basin (de Castro et al., 2012), such as the Afonso Bezerra Fault System (ABFS). The sedimentary deposits formed during the rift phase varied from fluvial, lacustrine, and fandeltaic (from the Pendências Formation) to deltaic and fluvio-deltaic units (from the Alagamar Fm) (Araripe and Feijó, 1994; Pessoa Neto et al., 2007).

The post-rift stage occurred in the early Albian, resulting from the breakup and opening of the seafloor (Fonseca et al., 2024). This stage involves thermal subsidence and the deposition of continental and marine sediments from the Alagamar Fm (Pessoa Neto et al., 2007). During the early Albian—Holocene, the drift phase was characterized by reduced subsidence rates driven by thermal and isostatic mechanisms (Bertani et al., 1990). This last stage included transgressive and regressive marine deposits (the Campanian-Maastrichtian Açu Fm), and represents the transition from fluvial-estuarine to marine environments, overlaid by the tidal-dominated carbonate shelf (the Turonian—Campanian Jandaíra Fm) (Pessoa Neto et al., 2007). The major unconformity marks the shift to transgressive deposits, which include the Barreiras, Tibau, Guamaré, and Ubarana formations, composed of siliciclastic to carbonate units (Pessoa Neto et al., 2007). These deposits reflect environments ranging from coastal fans, shallow platforms, and slope settings (Araripe and Feijó, 1994). The Afonso





Bezerra fault exhibits strike-slip and normal kinematics, affecting the rift and postrift units, where circulation of Si-rich fluids occurred (Menezes et al., 2019).

Three significant magmatic events shaped the basin: Rift-related dikes date back to ~132 Ma (Pessoa Neto et al., 2007), while alkaline basalt spills from the Cuó Volcanism occurred around ~93 Ma (Souza et al., 2004); and during the Eocene/Oligocene the Macau Fm that represents later intrusions striking to N-S (50–6 Ma) (Souza et al., 2019).

On the surface of our study area, the top of the pipes structures was described before as a silicified fault zone (ABFS segment) in the lower carbonate unit of the Potiguar Basin. This fault zone is complex and wide (up to 800 m), featuring multiple episodes of silicification and brecciation. The silicified zone includes partially silicified areas (angular fragments in a non-silicified carbonate matrix) and fully silicified zones; the latter are subdivided into low-porosity (no vugs) and high-porosity (with centimeter-scale vugs along fractures) sections. Silicification completely replaced the carbonate mineralogy with quartz, chalcedony, and opal, significantly increasing SiO₂ content (from 3–15% to 94–97%) (Menezes et al., 2019). This study highlighted the heterogeneity of the fault zone, where dynamic (syn-tectonic) and static (non-deformational) silicification processes coexist, influencing reservoir quality.

E.G. CRATERS, HOWN
ON FINNWALES

3. DATA AND METHODS

205 3.1 DATA





The study area encompasses 57 km² of the onshore Potiguar Basin (Fig. 2B). Subsurface data, including seismic and well logs, were provided by the National Agency for Petroleum, Natural Gas, and Biofuels (ANP). We used seismic reflection data from a 3D seismic survey and two 2D seismic lines. Data from one well were used in this study to perform a seismic-to-well tie for seismic interpretation. The well contains check-shot data and is located near one of the 2D seismic lines (Fig. 2B). The 2D seismic line passes through the well data with check-shot information. The 3D survey has 429 inlines and 554 crosslines, where these lines are oriented with NW-SE and NE-SW directions, respectively. The seismic cube extends down to a 3002-ms with a 4ms sampling interval and is prestack time-migrated. The 2D seismic lines were used in the lithostratigraphic interpretation to transfer the well-lithostratigraphic information (Açu Fm and basement tops) to the seismic cube area (Fig. 2).

3.2 Attributes analysis

To extract more information from the main reflectors, various attribute analyses have been performed (e.g., Chopra and Marfurt, 2007). Three main attributes have been applied: variance, cosine of phase, and dip illumination.

The variance attribute is a coherence attribute and is also considered a reverse version of semblance, which has been used in previous applications to indicate seismic breaks (lacopini et al., 2012; Liao et al., 2019, 2020; Phillips et al., 2019; Oliveira et al., 2023). These attributes calculate the similarity of seismic waveforms between adjacent traces (time-lagged cross-correlation in both inline and crossline directions) by estimating the coherence coefficient (Chopra and Marfurt, 2007). Variance can therefore reveal differences between seismic traces





and transform a continuity volume into a discontinuity volume, highlighting structural and stratigraphic boundaries (Brown, 2004; Mituku and Omosanya, 232 2020).

The cosine of phase attribute (Taner et al., 1979) is derived from the instantaneous phase of the seismic signal and represents the cosine of the phase angle. Unlike amplitude, the cosine of phase is less sensitive to amplitude variations, rather emphasizing phase-related changes in the seismic signature. The present study utilizes this attribute to reveal the lateral continuity between hydrothermal vents and the surrounding layers. The literature has extensively discussed the use of this attribute in the exploration of subtle discontinuities and mapping reflector continuities (Barnes, 1996; Chopra and Marfurt, 2007), which has been applied to improve the interpretation of various geological features, such as channels (Sarhan and Safa, 2017).

We did use the dip illumination attribute (Wu and Chen, 2006), and this seismic attribute simulates an illumination pattern revealing dip structure in the timeslice and can highlight these dip differences, using shine or color variation effect on a seismic map. Dip illumination is often used to detect structural features such as faults, folds, and fractures in the rotated layers of seismic lines (Lisle, 1994; Hesthammer and Fossen, 1997). The attribute is very efficient on time slices, and geological features are revealed when this attribute defines a reflective surface on which a discontinuity measure is estimated (Chopra and Marfurt, 2007). We used the dip illumination attribute to support the location and mapping of each fluid pipe previously highlighted by the variance answer, which enhances the scatter and discontinuities. The fluid pipes were then extracted into





bodies by isolating the variance answer, allowing the hydrothermal vents to be visualized in a 3D perspective.

3.3 Apparent Aspect Ratio (ARA)

We used the Apparent Aspect Ratio (ARA), which is a quantitative measure used to assess the plan-view geometry of fluid escape pipes identified in 3D seismic data (Maestrelli et al., 2017). It is defined as the ratio between the lengths of the long and short axes of a pipe's cross-section, measured along seismic inlines and crosslines. Since these directions may not align with the true maximum and minimum dimensions of the structure, the resulting value is only an approximation of the actual elongation. For this reason, it is referred to as "apparent" and cannot be directly used to infer regional stress orientations. Despite this limitation, the ARA is useful for distinguishing between circular and elongated pipe geometries. Values close to 1 indicate pipes with a nearly circular shape, while higher values suggest elliptical or more elongated forms in plan view. This distinction can provide important insights into the morphology and potential development mechanisms of these features.

To calculate the ARA, measurements are performed on cross-sections extracted from the seismic volume, typically at two different heights along the pipe: one near its base and another closer to its upper termination. The long and short axes are determined using orthogonal seismic slices—inline and crossline directions—intersecting the pipe at those levels. The ratio between these two axes yields the ARA value for that section. Pipes displaying highly irregular, coalescing, or interacting geometries are excluded from analysis due to the difficulty in defining consistent axis lengths along their conduit.

https://doi.org/10.5194/egusphere-2025-3487 Preprint. Discussion started: 16 September 2025 © Author(s) 2025. CC BY 4.0 License.





4. RESULTS

4.1 Mapping by conventional seismic interpretation

The study area comprises part of the onshore Potiguar Basin, featuring a post-rift seismic unit and basement rocks. Two lithostratigraphic formations (Açu and Jandaíra) are identified and described above the basement reflector (Fig. 3B). The basement exhibits discontinuous, scattered reflectors, with its top marked by green dots (Fig. 3b). This seismic facies is characterized by continuous reflectors often disrupted by mound-like or convex structures intruding the overlying unit, displaying strong amplitude anomalies. The Açu Fm, directly overlying the basement, shows a coherent, homogeneous reflection pattern intersected by straight columnar units (Fig. 4b) and diffuse structures with poorly defined boundaries (Fig. 4a). The Jandaíra Fm, above the Açu Fm, displays more continuous and homogeneous facies, interrupted by diffuse low-amplitude anomalies. These amplitude anomalies present patchy disruptions in both horizontal and vertical continuity. In seismic lines, these patches appear as intrusive facies with chaotic reflectors cutting across the primary layering.



296



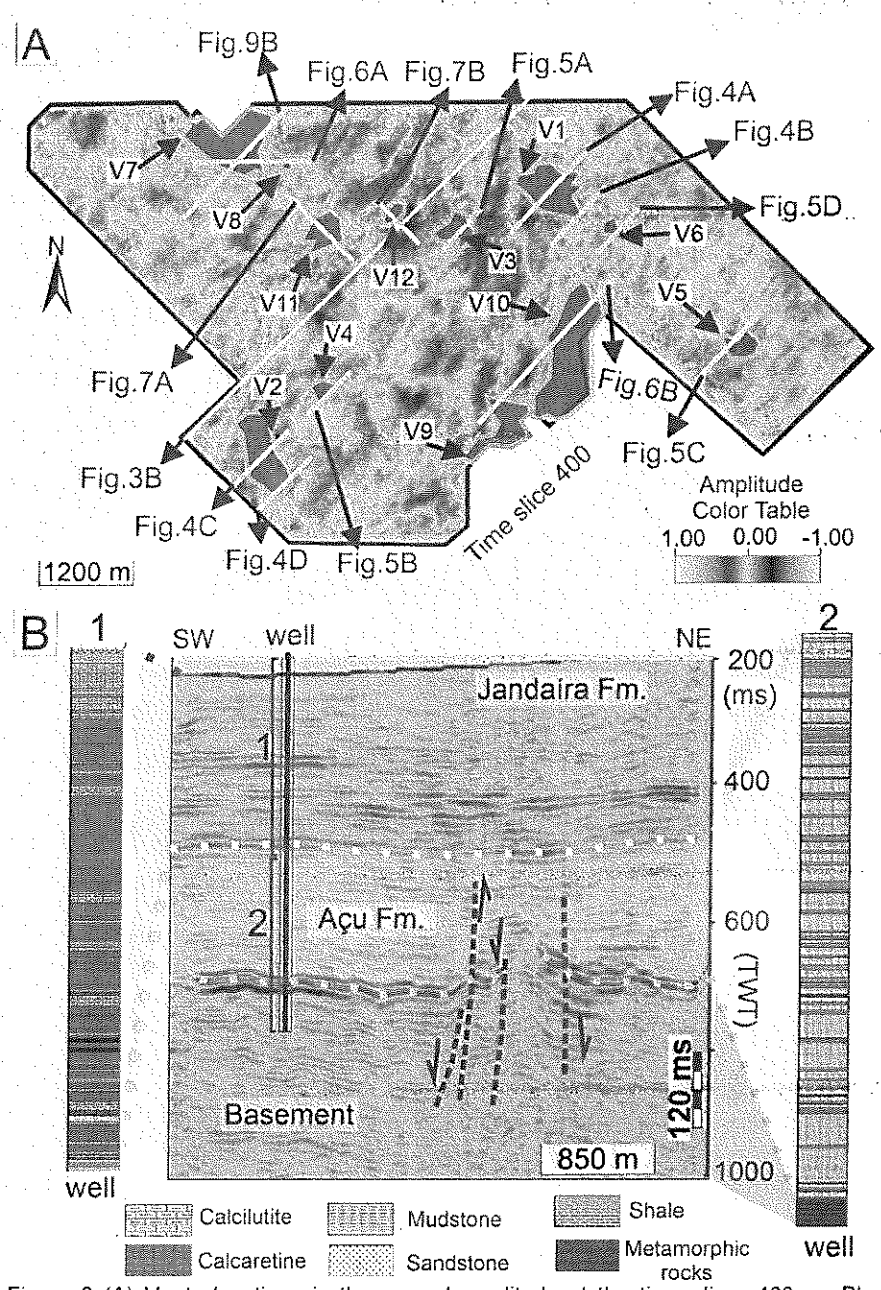


Figure 3 (A) Vents locations in the normal amplitude at the time slice -400ms. Blue shapes represent vents shapes. Yellow tines – seismic sections interpreted location in





this study. V - Vents . (B) Lithostratigraphic interpretation of a vertical section based on the well data. Vertical exaggeration: 5x.

The discontinuous basement reflectors suggest a highly fractured or heterogeneous igneous/metamorphic basement. The mound-like intrusions and amplitude anomalies may indicate igneous bodies or fluid migration pathways. The Açu Fm columnar and diffuse structures likely represent sedimentary deposits influenced by syn- or post-depositional intrusions. The chaotic patches in the Jandaíra Fm imply secondary processes such as fluid expulsion or soft-sediment deformation.

4.1.1 Characteristics of the hydrothermal vent complex

We characterized the main columnar vertical seismic facies intruding the main seismic package presenting deteriorated seismic signal, so the primary reflections either are absent or very weak (we will call thereafter those zones as wipe out zone, sensu Loseth et al., 2004) showing also edge discontinuities and attenuation of the reflectors (Figs. 4, 5, 6, and 7). Both along inlines or crosslines, some of these structures are represented by wipe out zones rimmed by an inner zone of high amplitude anomalies and an outer zone of dim amplitude anomalies. The various wipe out zones probably reflect various types of leakage processes through the low-permeable zone, contrasting with the surrounding reflector packages, where the disturbed zones stand out from the surrounding horizontal reflectors (Fig. 4a,b, and 6a,b). Therefore, other seismic sections show instead a more localized signal disturbance (Fig. 4c,d, and Fig. 5a,b), related to the leaking from fault structures. In Figures 7a and b, we observe a large disturbance zone broadening upward, making the signal interpretation near the surface difficult. Interestingly almost all figures show within all columnar areas of the disturbance

https://doi.org/10.5194/egusphere-2025-3487 Preprint. Discussion started: 16 September 2025 © Author(s) 2025. CC BY 4.0 License.





zone upward convex deflection of the main reflectors (Figs. 4, 5, 6, 7). This
horizon deflection has been observed, except in some rare cases, with a different
degree of development. In some of the largest examples with large wipe out zone,
a chaotic expression of the seismic signal is visible: the reflection terminations of
the deflected horizons show a clear loss of amplitude and a disruption of the
internal architecture of the pipe.





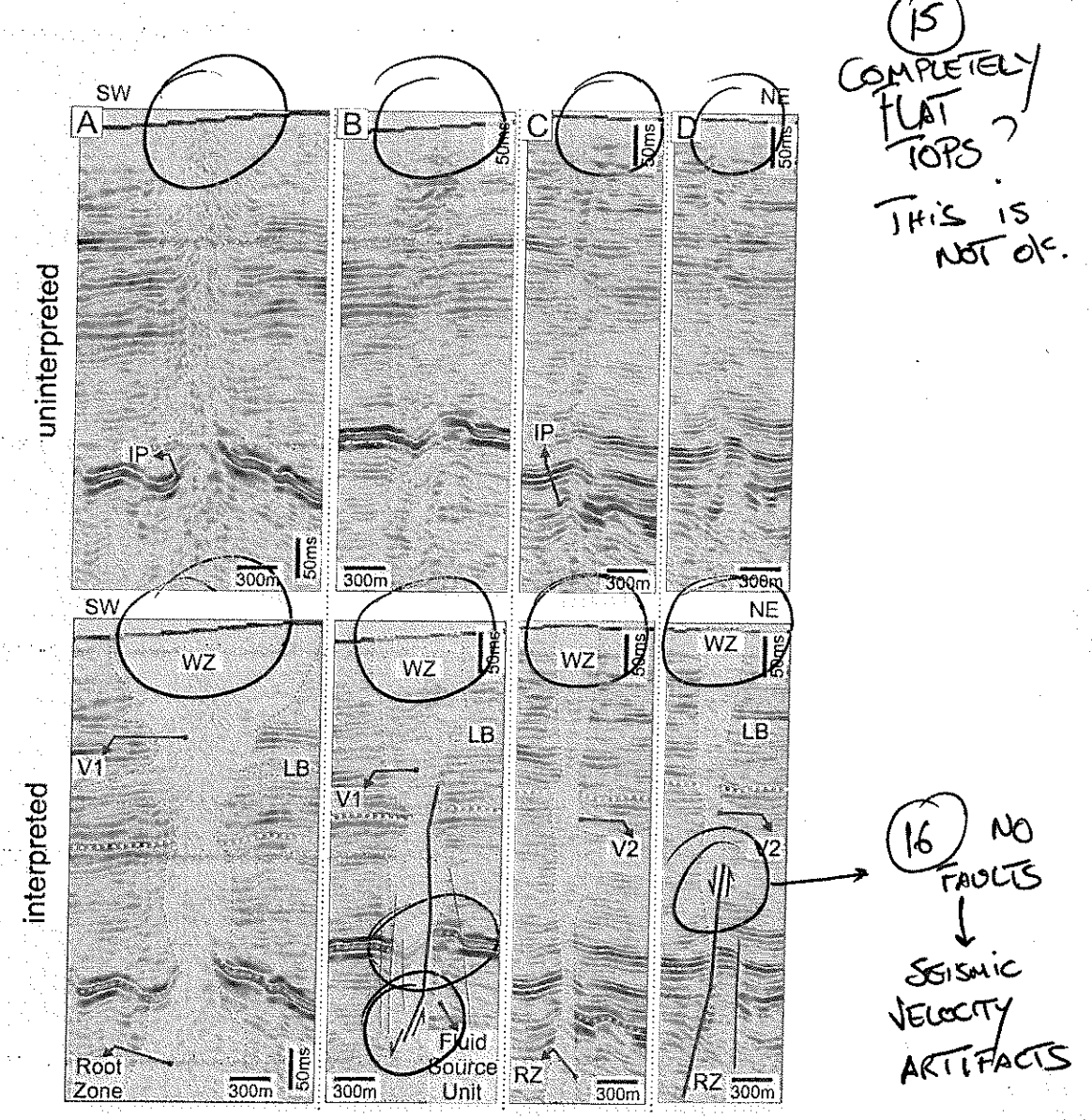


Figure 4 - Characterization of the vents 1 and 2 (V1 and V2) with their elements: Wipe out Zone (WZ). Dead Mixed Zone (DMZ), Inflection Point (IP), and Lateral Brightness (LB). When the vertical disturber zone is surrounded by bright reflectors, we refer to wipe out zone. Yellow dotted lines - Açu Fm top, green dotted lines - Basement top. Vertical exaggeration: 5x.

The root zone indicates the fluid source unit, which is below the basement top, and shows that those columnar wipe out zones are connected below the basement top. In the more localized condition the wipe out zone is exploiting





- individual normal faults (Figs. 4, 5, 6, and 7). In our study case, all those columnar 337
- seismic facies are often connected to faults showing a normal fault kinematic. 338

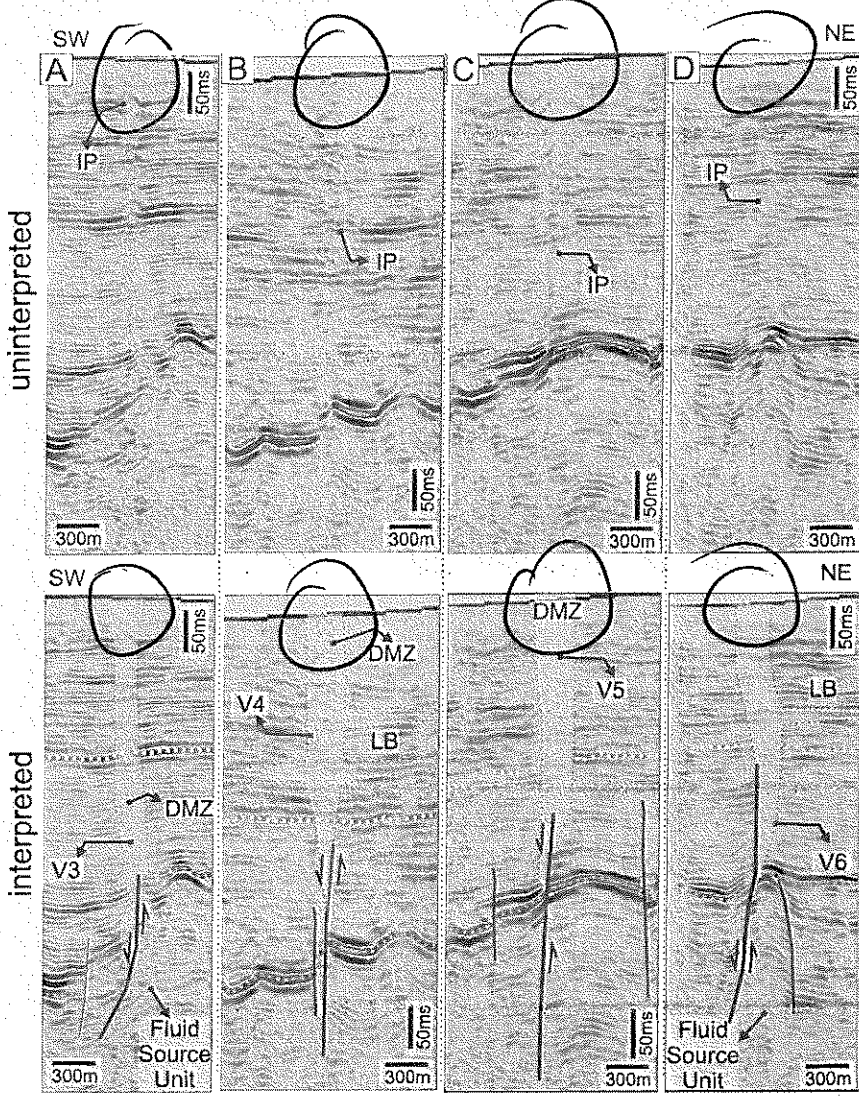


Figure 5 - Characterization of the vents (A) 3, (B) 4, (C) 5, and (D) 6 (V3, V4, V5, and

V6) with their elements: Dead Mixed Zone (DMZ), Inflection Point (IP), and Lateral Brightness (LB). Yellow dotted lines - Açu Fm top, green dotted lines - Basement top. Vertical exaggeration: 5x.

342 343

339

340

341

https://doi.org/10.5194/egusphere-2025-3487 Preprint. Discussion started: 16 September 2025 © Author(s) 2025. CC BY 4.0 License.





Inside the main columnar wipe out zones, we can characterize some further seismic details (V1, V7, V10). The WZ, which are disturbed and chaotic zone, creates a zone of amplitude points or semi-continuous reflectors (Figs. 4, 6, and 7). The presence of inflection point (IP) of the seismic reflectors affecting the beddings, producing reflectors with dome-shaped, suggesting push-ups, which suggests a clear velocity changes in the seismic signal (Figs 4,5,6).





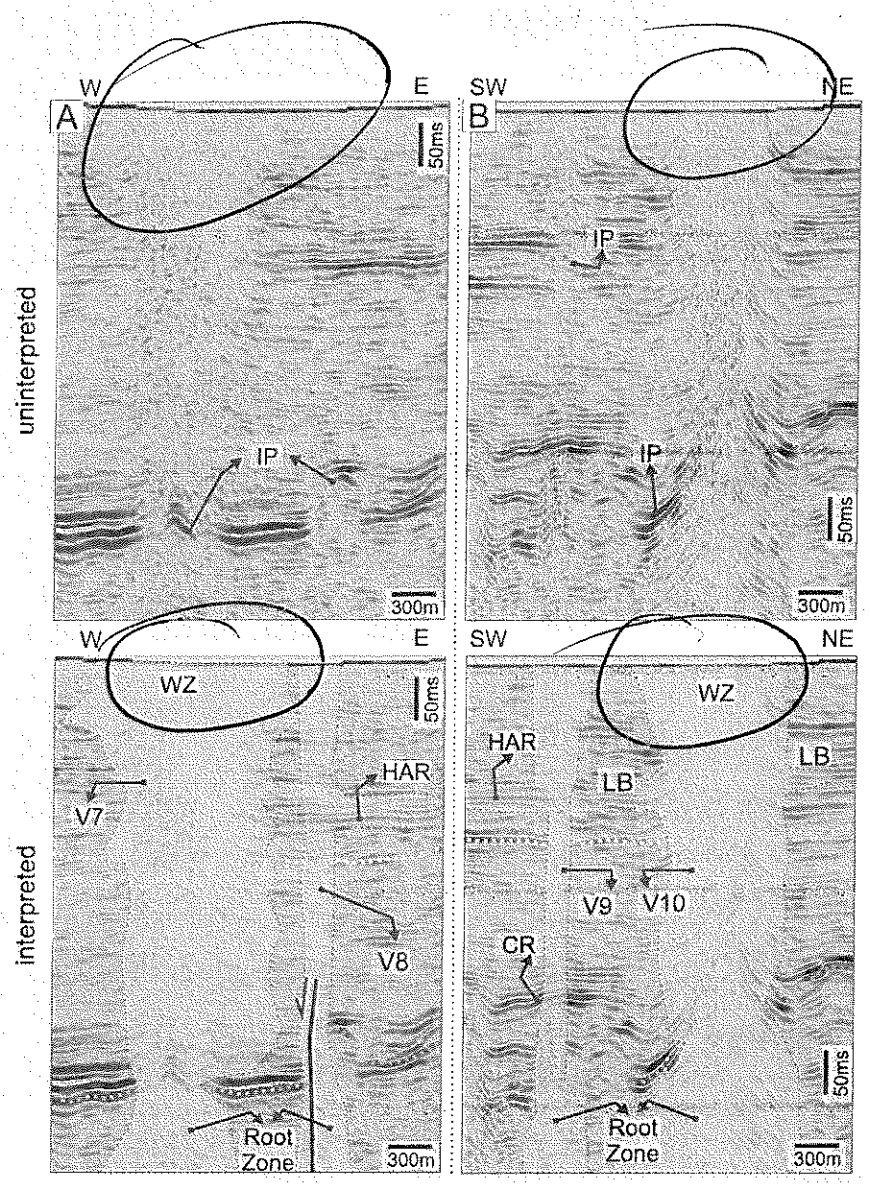


Figure 6 - Characterization of the (A) vents 7 and 8 (V7 and V8) and (B) vent 9 (V9) and 10 (V10) with their elements: Wipe out Zone (WZ), Inflection Point (IP), Lateral Brightness (LB), High Amplitude Reflectors (HAR), and Coherent Reflector (CR). Yellow dotted lines - Açu Fm top, green dotted lines - Basement top. Vertical exaggeration: 5x.

The columnar wipe out zones with a 'downward tapering cone' (V1, V7, and V10) increase their width through the top, crossing all the formations of the basin up to the surface (Figs 4, 5, and 6), making it impossible to characterize

https://doi.org/10.5194/egusphere-2025-3487 Preprint. Discussion started: 16 September 2025 © Author(s) 2025. CC BY 4.0 License.





- 358 the vents terminus in our study area. Close to all pipes, we do recognize high
- amplitude reflectors (HAR) and increasing their lateral brightness (LB) (Figs. 4,
- 360 5, 6, and 7).





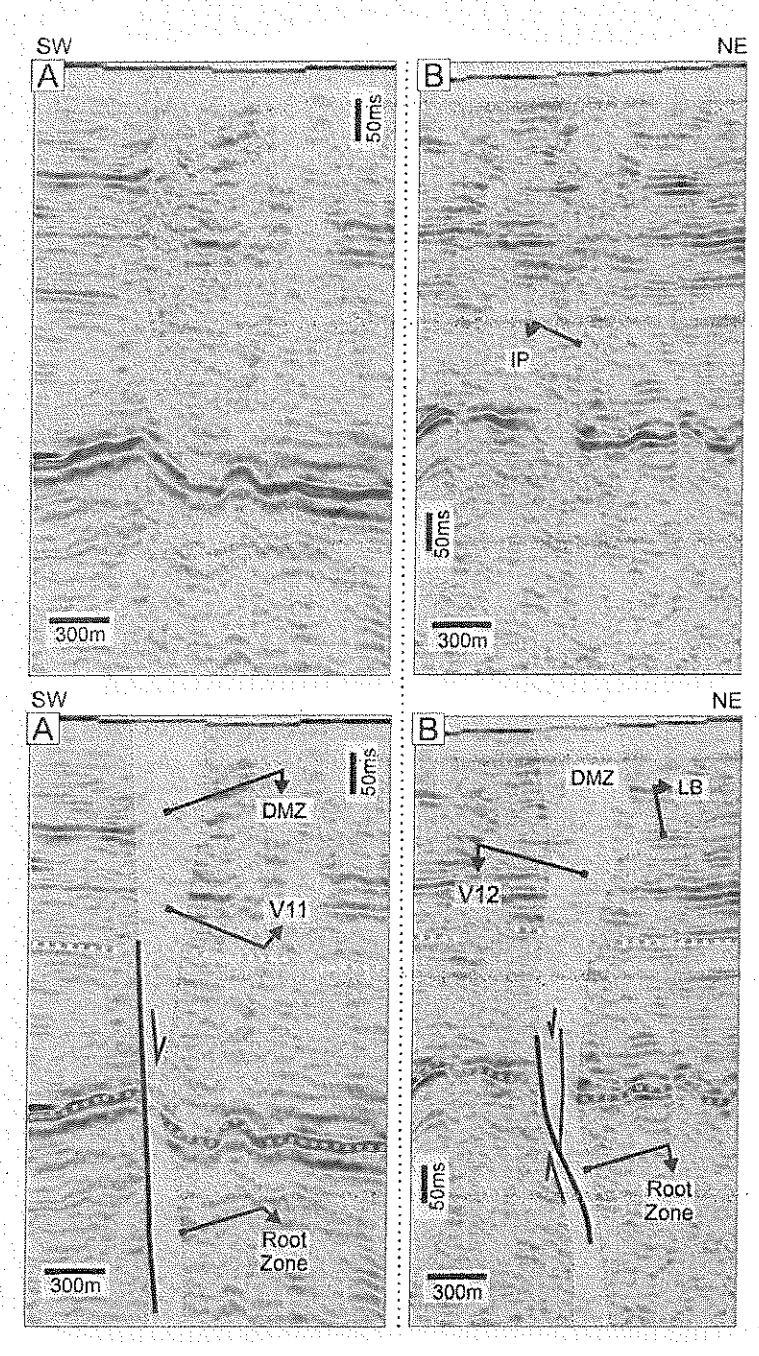


Figure 7 - Characterization of the fluid pipes 8 and 9 (P8 and P9) with their elements: Dead Mixed Zone (DMZ), Inflection Point (IP), and Lateral Brightness (LB). Yellow dotted lines - Açu Fm top, green dotted lines - Basement top. Vertical exaggeration: 5x.

22





4.2 Seismic Attributes

The application of seismic attributes such as dip illumination (Fig. 8B) and variance (Fig. 8C) confirms and enhances the signal anomalies corresponding to the wipe out zones, correlated to the vents, and to structures such as faults and fractures in their zones (Fig. 8D and E).

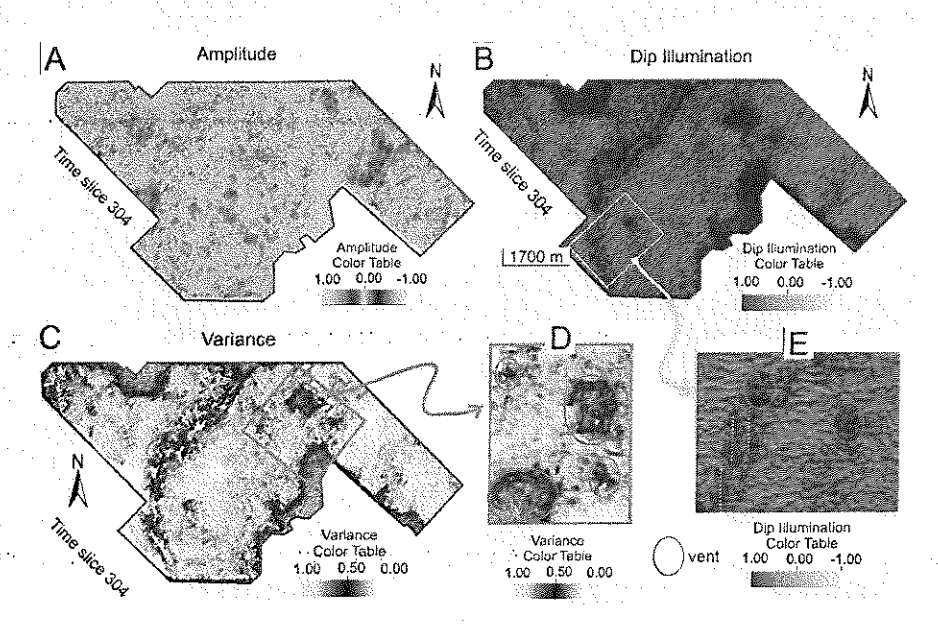


Figure 8 - Comparison of the seismic answers between (A) amplitude, (B) dip illumination, and (C) variance, revealing (D) the vents or fluid pipes and (E) the surrounding structures at the time slice 304ms. White dotted line – fault traces.

In vertical sections, the variance answer cover a large area of the wipe out zone related to the vent structures and cover entirely the dead mixed zones from the fluid pipes (Fig. 9). The variance attribute completely covers the fluid pipe shapes with low width variation (Fig. 9) and loses some areas for the vents with a conical shape (Fig. 9B). This correspondence between the variance attribute and the dead mixed zones provides an automatic vertical characterization of the pipes. The variance attribute reveals areas related to the



vents and fluid pipes, showing a great correspondence compared with the manual interpretation of the vents, which is observed by combining the variance answer with the normal amplitude for the pipes.

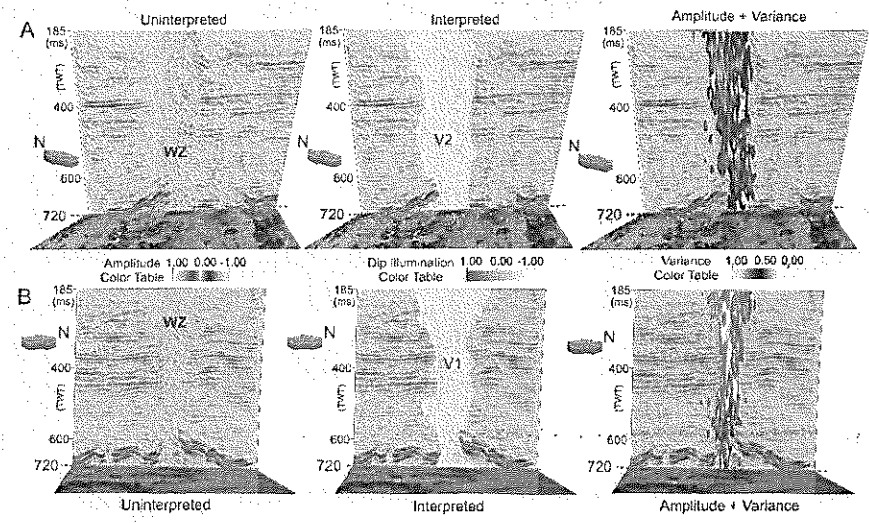


Figure 9 - External shape comparison between normal amplitude uninterpreted, interpreted, and variance attribute applied for the pipes V2 (A) and V1 (B). See Figure 3A for the location of the vents. Vertical exaggeration: 5x.

Even though applying the variance attribute is very effective in recognizing and characterizing hydrothermal vents, the vertical continuity of some fluid pipes can not be delimited (Fig. 10A and B). With the application of the cosine of phase attribute, the vertical and lateral continuity of the pipe anomalies caused by the seismic signal becomes more visible due to the contrast between the seismic facies pattern of the hydrothermal vents and the host rock. For some pipes, the shape of a 'christmas tree' becomes evident with the application of the cosine of phase (Fig. 10C), highlighting the variation in the lateral distribution of the fluid into the sedimentary formations.





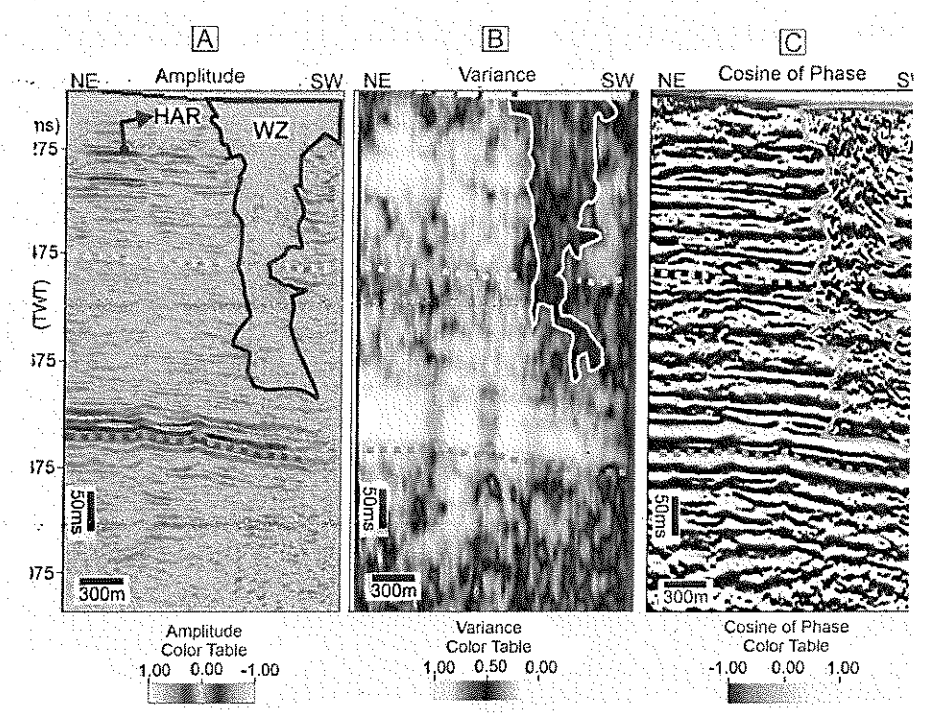


Figure 10 - Comparison of the pipe (V2) external shape between the normal amplitude (A), Variance (B), and Cosine of Phase (C) interpretation in a vertical section. See Figure 3A for the location of the vents. Vertical exaggeration: 5x.

Applying the cosine of phase attribute highlights the reflectors affected by the fluid, where the wipe out zone connect or penetrate the sedimentary formations of the basin (Fig. 11). The application of the cosine of phase attribute shows a new geometry of these structures, which are much more complex fluid bodies in a 3D perspective than previously highlighted by manual interpretations or compared to the variance attribute application.





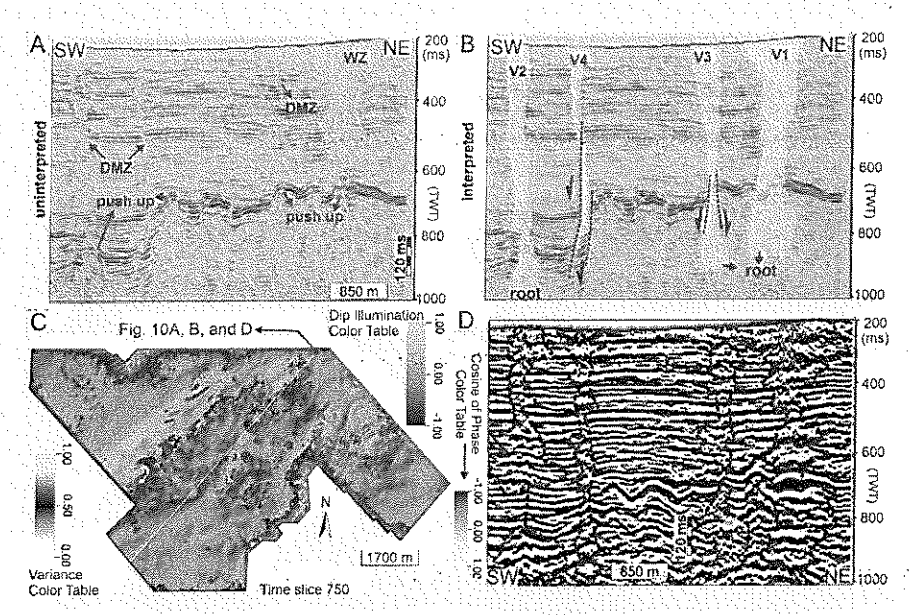


Figure 11 – Comparison between the fluid bodies geometry in (A) an uninterpreted vertical section, (B) with a manual interpretation of the vents and fluid pipes. (C) Time slice 750 ms applied Dip Illumination and Variance. (D) The cosine of phase attribute applied in the same seismic section. Vertical exaggeration: 5x.

4.3 Structural and geometric analysis of the wipe out zones

DIM (

PONES.

We chose two wipes out zones to analyze the geometric parameters of the external shape. The graph of the pipes' geometrical parameters consisted of the values of the wipe out zones axes 1 and 2, in the direction of the inlines and crosslines (Fig 12B), as well as the apparent aspect ratio by measuring the maximum and minimum fluid structures axes (Fig. 12C). All the values were measured at different depth levels from the fluid structures geobodies based on the variance attribute (Fig. 12A). We choose to show the values in a graphs with a fixed horizontal axis due the comparison between wipe out zones results.

The values measured above the inlines are higher for both fluid structures (V1 and V2), which are, therefore, more elongated in the NW-SE direction. For V1, the values of the axes in the inline and crossline directions are close to each

431 432

433

434

435

436

437

438

439

other (from 120m to 820m) in the inline direction, thus showing more dispersion of the data on the graph (Fig. 12B). The smaller axis of the V2 pipe is in the direction of the crossline (NE-SW) where its values vary from 120 to 450 m.

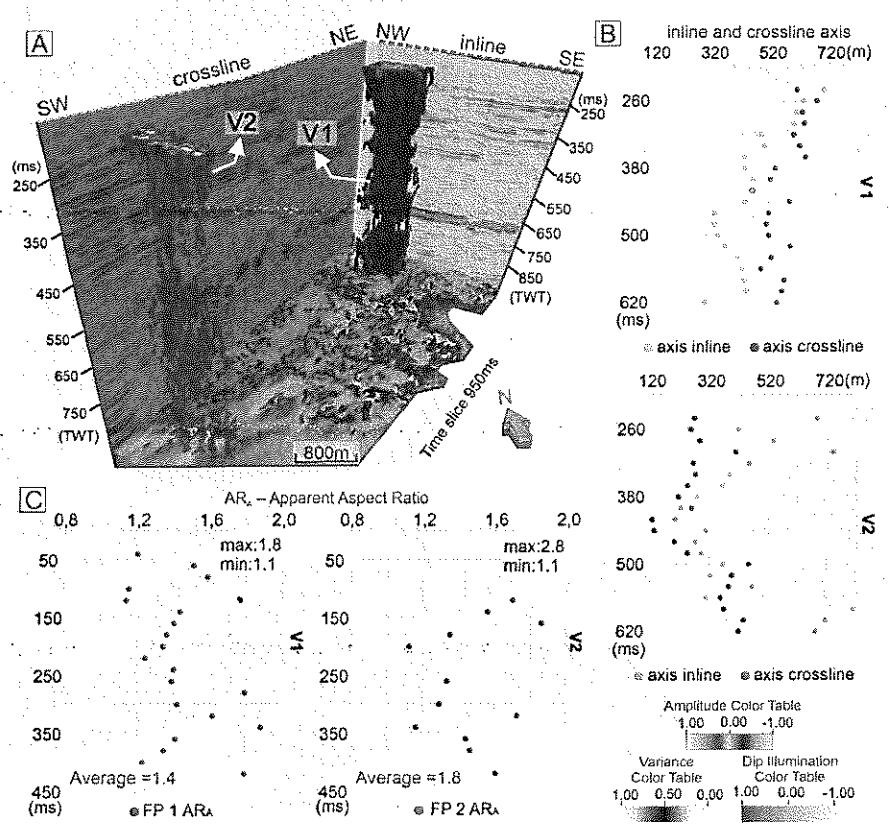


Figure 12 - (A) Geobodies of the vents 1 and 2 extracted based on the variance attribute. The graphs display the fluid pipe axis in inline and crossline directions (B) and their Apparent Aspect Ratio (ARA) to understand the fluid structures ellipticity in different levels. Vertical exaggeration: 5x.

We used the ARA to verify the ellipticity of the fluid structures. Based on Maestrelli et al. (2017), the apparent aspect ratio (ARA) was calculated as the ratio of the long axis to the short axis, approximating the pipe's elongation in plan view (circular if ARA \approx 1, elliptical if ARA > 1). The values calculated from the maximum and minimum axes for the apparent aspect ratio exhibit greater





dispersion for the V2 pipe, with the opposite behavior observed in the V1 graph
(Fig. 12C). The maximum radius values for V2 reach 2.8, which is 2 times the
length of V1, with values of 1.8. This demonstrates a strongly elliptical
classification of both pipes, with an ARA average of 1.4 and 1.8 for V1 and V1,
respectively. With this, the axis elongation striking to NW-SE for both pipes shows
a greater directional control in the V2 values.

5. DISCUSSION

446

447

448

449

450

451

452

453

454

455

456

457

458

459

460

461

462

463

5.1 Geometry of the hydrothermal vents complex and fault systems

Previous studies associate hydrothermal vent complexes with faults, describing them as pipe fault-related (Planke et al., 2005) or fluid conduits (Magee et al., 2014; Rovere et al., 2014), often linked to structures above and around vents (Hansen, 2006; Kjoberg et al., 2017) or gas ascent within polygonal fault systems (Rovere et al., 2022). Our seismic analysis identifies "wipe-out zones" and "dead mixed zones" (Figs. 4-7), characterized by reflectors attenuation and internal chaotic pattern, and revealing that all analyzed pipes are associated with fault activity. This suggests their formation cannot be attributed solely to hydraulic fracturing or igneous intrusion-related pressure (Skogseid et al., 1992; Davies et al., 2002, 2012; Aarnes et al., 2010). Our description shows these vents are structurally controlled by regional faults, with root zones extending below the basement, indicating a fluid source within the crystalline basement. Surface studies by Menezes et al. (2019) corroborate this, showing the NW-SE Afonso Bezerra Fault System (active from rift to post-rift phases) cutting through the basin and basement. Seismic interpretation further reveals fluid conduits elongated along fault trends (Figs 12), with "inflection points" (IP)





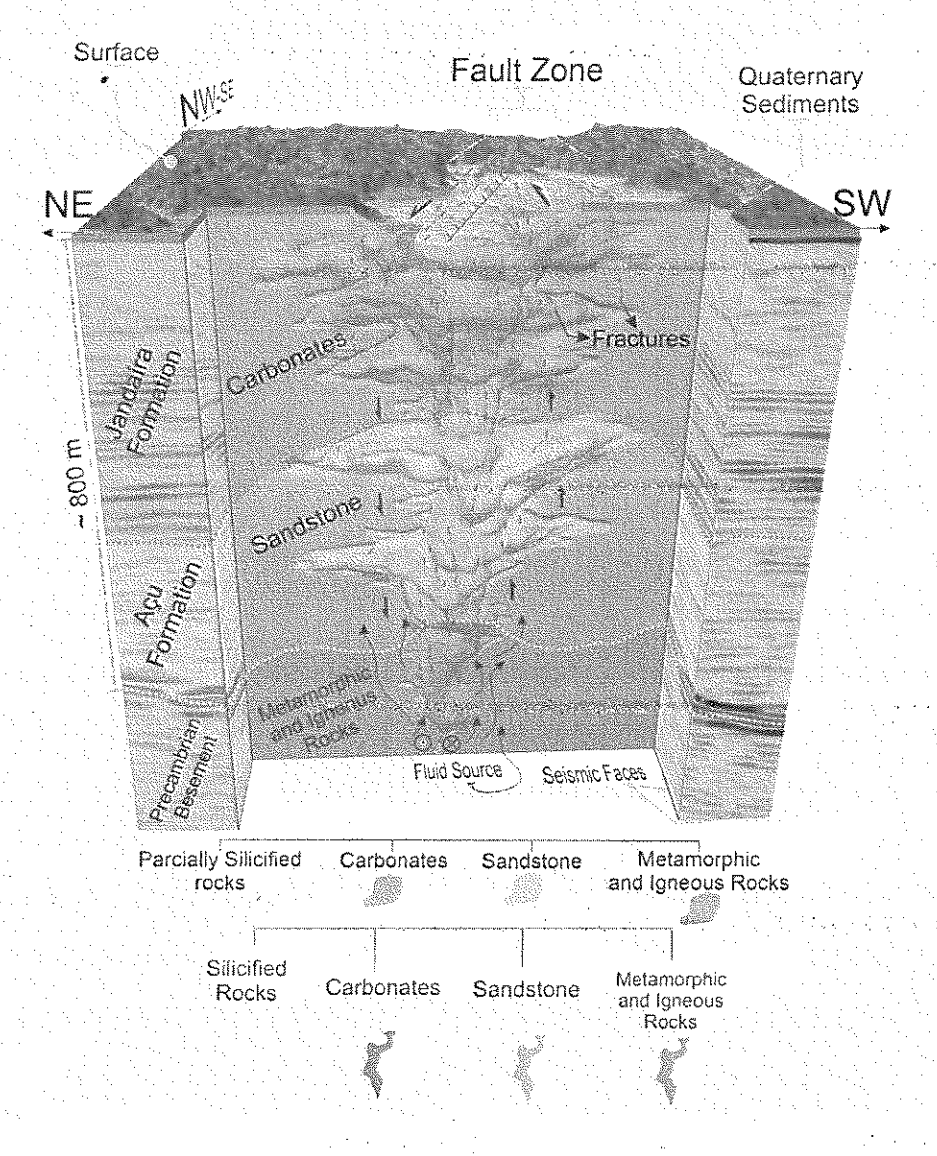
forming dome-shaped geometries (Figs. 4–7), indicative of fluid ascent altering sedimentary layers. The internal signal and edge reflectors related to the vents show a push-up geometry, mostly dragging upward the main reflector (Figs. 4, 6, and 11), which suggests a denser intrusive unit, distinguishing it from a simple gas intrusion. Therefore, this is typical of hydrothermal rock or intrusion, which produces mineralization often re-fractured but the various intrusions. These conduits align with surface silicified breccias (Menezes et al., 2019), confirming their hydrothermal origin. Additionally, magmatic activity in the Potiguar Basin (e.g., Macau and Serra do Cuó events; Mizusaki et al., 2002; de Castro et al., 2012; Souza et al., 2019) likely contributed to thermal anomalies and sedimentary alteration, facilitating vent genesis.

The application of the cosine of phase attribute with the lateral brightness recognition (see LB in Figs. 4A, B, C, 5B, D, 6B, and 7B) reveals the vent fluids entering laterally in the sedimentary layers, changing the vents geometry (Fig. 13). The interaction between hydraulic fracturing, overpressure, and faults must be considered for a more comprehensive understanding of the genesis of the pipe systems, since structures as faults change the permeability influencing fluid flow (Caine et al., 1996; Faulkner et al., 2010; Palhano et al., 2023), acting as seals or conduits (Fisher et al., 1998; Bense et al., 2013; Torabi et la., 2021; Medici et al., 2021; Labry et al., 2025). Although previous studies suggest that hydraulic fracturing is a fundamental mechanism for the initiation and control of vent formation (Svensen et al., 2006; Alvarenga et al., 2016), we highlight that the development of brittle structures such as faults plays a crucial role in this process (Fig. 13). This implies that the evolution of the vents should be





- 488 interpreted in a broader tectonic context, where faults act as preferential
- pathways for fluid migration and control their ascent and escape.



490 491

- Figure 13 The schematic model of fluid pipes ascending through the sedimentary basin controlled by a fault. Red traces fractures.
- Sedimentary basins that feature fluid pipes or hydrothermal vents, such
- as those in the Gulf of Mexico (Roberts and Carney, 1997; Aharon, 1994), the





North Sea (Cartwright et al., 2007; Løseth et al., 2009), the Santos Basin (Camboa and Rabinowitz, 1981; Mohriak et al., 2008), and the Campos Basin (Guardado et al., 1989; Bruhn and Walker, 2006), are characterized by dynamic geological systems where the circulation of thermal fluids plays a crucial role in rock modification and the generation of petroleum systems (Palhano et al., 2023; Maciel et al., 2024). In these basins, fluid pipes are often associated with tectonic and magmatic processes, creating migration pathways for hydrocarbons and contributing to the formation of structures such as sandstone dykes and hydrothermal alteration zones.

5.2 Seismic data limitation in the vents characterization

The hydrothermal vents are described in their parts as inner and outer zones based on the composition and structures of the vent outcropping, and how they affect the host rock (Jamtveit et al., 2004; Svensen et al., 2006). These vent zone descriptions allow the characterization of the fluid zones in terms of origin, host rock permeability, fluid pressure, and pipe complexity (Planke et al., 2005), where these zones were measured and analyzed using field data in previous studies. In the literature, major hydrothermal vent complex characterization has been conducted using seismic data by applying coherence attributes to reveal these structures (Svensen et al., 2003; Hansen, 2006; Kjoberg et al., 2017; Wang et al., 2019). In our case, we used seismic attributes such as variance, dip illumination, and cosine of phase to distinguish the disturbed zones from the fluid pipes and the host rock in the seismic data (Figs. 8, 9, 10, and 11), but even with this, it is impossible to define the internal vent zones as other previous studies (McDonnell et al., 2007; Magee et al., 2016; Mituku and Omosanya, 2020; Chen



520

521

522

523

524

525

526

527

528

529

530

531

532

533

534

535

536

537

538

539

540

541

542

543



et al., 2021). Therefore, the data resolution still limits the characterization of fluid pipe zones in the seismic data.

Coherence attributes alone can highlight other geological features besides faults (e.g., channel edges) or artifacts, and therefore need to be geologically validated. In our fluid pipes interpretation, it is evident that the fluid pipe detection in seismic data and the seismic attributes applied, such as variance and dip illumination, are particularly sensitive to these discontinuities (Figs. 8, 9, 10, and 11). We used seismic data from a shallow sedimentary package of the Potiguar Basin onshore portion, which presents noise or NR areas close to the surface or inside the basement, making the geometric characterization of the vents difficult. Among various seismic attributes, those that emphasize discontinuities between seismic reflectors or geological horizons are the most suitable ones for imaging faults (Chopra and Marfurt, 2005; Di et al., 2019, Libak et al., 2017; Oliveira et al., 2023) and vent complex areas as disturbed zones. However, the presence of noise poses a significant challenge and is very impacted to noise and no disturbance of the reflectors, as it can adversely affect the accuracy and reliability of seismic attribute results (Cohen et al., 2006; Hale, 2013; Wu et al., 2019).

6. CONCLUSIONS

Our results demonstrate that hydrothermal vent development in the Potiguar Basin is fundamentally controlled by fault activity, particularly the Afonso Bezerra Fault System. The strongly elliptical and elongated vent geometries aligned with fault trends contribute to the previous models that attribute vent formation solely to hydraulic fracturing from igneous intrusions. Instead, we propose a hybrid model where faults act to guide the fluid pathways, modify



545

546

547

548

549

550

551

552

553

554

555

556

557

558

559

560

561

562

563

564

565

566 567

568

569 570



permeability, and change the vent morphology. Fault zones not only localize vents but also enhance reservoir-scale permeability, with implications for hydrocarbon migration and hydrothermal mineralization. The association of vents with regional fault systems suggests their formation is intrinsically linked to the basin's rift-related tectonic framework. This aligns with global analogs (e.g., Gulf of Mexico, North Sea), where vents develop along fault zones in magmatically active basins. The Potiguar Basin's silicified breccias and magmatic events (e.g., Macau and Serra do Cuó) further support a tectonic-magmatic interplay in the vent development. While seismic attributes (variance, dip illumination, and cosine of phase) effectively delineate vent boundaries and disturbed zones, they cannot resolve internal vent zonation (e.g., inner/outer zones) observed in the field studies. Discontinuity-based attributes (e.g., coherence) are sensitive to vent structures but require geological validation to distinguish vents from other features. Variance and dip illumination proved most robust for mapping fault-vent relationships. though noise in shallow sedimentary sections limits geometric precision. Data resolution and near-surface noise remain key challenges, emphasizing the need for integrated approaches combining seismic, well, and outcrop data. **Author Contribution** L. S. B.O.: Conceptualization; Investigation; Methodology; Validation; Visualization; Roles/Writing - original draft; and Writing - review & editing L.C.V.L.: Conceptualization; Investigation; Methodology; Visualization; Roles/Writing - original draft; and Writing - review & editing D.I.: Conceptualization Investigation; Methodology; Formal analysis; Validation; Visualization; Roles/Writing - original draft; and Writing - review & editing F. B.: Conceptualization; Investigation; Methodology; Supervision; Validation;

Visualization; Roles/Writing - original draft; and Writing - review & editing





A. T.: Conceptualization; Formal analysis; Investigation; Methodology; 571 Supervision; Validation; Visualization; Roles/Writing - original draft; and Writing 572 - review & editing 573 B. A.: Conceptualization; Formal analysis; Investigation; Methodology; 574 Supervision; Validation; Visualization; Writing - review & editing 575 J.F. de S.N.: Investigation; Methodology; Validation; Visualization; 576 P. E. F. M.: Visualization; Writing - review & editing 577 D. L. V.: Writing - review & editing; 578 579 V. La B.: Writing - review & editing; F. H. R. B.: Conceptualization; Investigation; Methodology; Resources; Project 580 administration; Supervision; Validation; Visualization; Roles/Writing - original 581 draft; and Writing - review & editing. 582 The authors declare that they have no conflict of interest 583 **ACKNOWLEDGES** 584 This research was carried out in association with the ongoing R&D project 585 registered as ANP 23505-1, "Processos e Caracterização de Rotas de Fluxo de 586 Fluidos em Reservatórios Carstificados, Fraturados e Silicificados do Pré-Sal -587 Porocarste Fase II" (UFRN/UNB/UFPE/UFC/UFRA/IFRN/IFPB/Shell Brasil/ANP) 588 - Porokarst Phase II - Processes and Characterization of fluid pathways in 589 Karstified, Fractured and Silicified Reservoirs of the Presalt, sponsored by Shell 590 591 Brasil under the ANP R&D levy. DLV thanks CNPq for its productivity grant (PQ 592 grant). 593 594 **REFERENCES** Aarnes, I., Svensen, H., Connolly, J.A., Podladchikov, Y.Y., 2010. How contact 595 metamorphism can trigger global climate changes: Modeling gas generation 596 around igneous sills in sedimentary basins. Geochim. Cosmochim. Acta 74 (24), 597

7179-7195. https://doi.org/10.1016/j.gca.2010.09.011.